

ON THE NUMERICAL SOLUTION OF A NONLINEAR EIGENVALUE PROBLEM FOR THE MONGE-AMPÈRE OPERATOR

Roland GLOWINSKI (University of Houston) & Hao LIU (Georgia Tech)

Dédié à François Murat pour ses contributions à l'analyse mathématique des équations elliptiques non linéaires dont

$$-\nabla^2 u = \lambda e^u$$

JL² LAB 50, March 2019

0. MOTIVATION

In the early 2000, while looking for *PDE's from Geometry*, I came across an article of *Alice Chang* discussing the *Laplace-Beltrami-Bratu-Gelfand* problem

$$\text{(LBBG)} \quad \Delta_{\Sigma} u + \lambda e^u = 0 \quad \text{on } \Sigma$$

where Σ is a surface of \mathbf{R}^d and Δ_{Σ} the associated *Laplace-Beltrami operator*. At the time I was more interested in the *Monge-Ampère equation*

$$\det \mathbf{D}^2 u = f(> 0) \quad \text{in } \Omega$$

where Ω is a *bounded convex domain* of \mathbf{R}^d . For some strange reason, **(LBBG)** became in my mind

$$\det \mathbf{D}^2 u = \lambda e^u \quad \text{in } \Omega$$

explaining what's follows (when I realized my mistake it was too late).

1. FORMULATION OF THE EIGENVALUE PROBLEM

Assuming that Ω is a *bounded convex* domain of \mathbf{R}^2 , our goal is to solve *numerically* the following *nonlinear eigenvalue problem*: (**Monge-Ampère-Bratu-Gelfand** problem)

(MABG) $\left\{ \begin{array}{l} \text{Find } u \text{ } \mathit{convex} \text{ and } \lambda > 0 \text{ such that} \\ \int \det \mathbf{D}^2 u = \lambda e^{-u} \text{ in } \Omega, \\ u = 0 \text{ on } \partial\Omega, \\ \int_{\Omega} (e^{-u} - 1) d\mathbf{x} = C(> 0). \end{array} \right.$

Above

$$d\mathbf{x} = dx_1 dx_2$$

REMARK 1. The *convexity* of Ω and u , and the condition $u = 0$ on $\partial\Omega \Rightarrow u < 0$ in Ω .

REMARK 2. P.L. Lions, *Annali di Matematica Pura ed Applicada*, 142(1), 1985 contains mathematical results associated with a closely related nonlinear eigenvalue problem (λu^2 instead of λe^{-u}).

REMARK 3. Suppose that Ω is the *unit disk* centered at $(0, 0)$. Looking for *radial solutions* to (MABG) we solve

$$(1) \quad \begin{cases} u \leq 0, \lambda \geq 0, \\ u'u'' = \lambda r e^{-u} \text{ on } (0,1), \\ u(1) = 0, u'(0) = 0, \end{cases}$$

(by a *shooting method* for example). The related *bifurcation diagram* has been visualized on **Figure 1**, below, showing a *turning point* at $\lambda \approx 3.7617$, the associated function u taking its *minimal value* at $(0, 0)$ with $u(0,0) \approx -2.5950$.

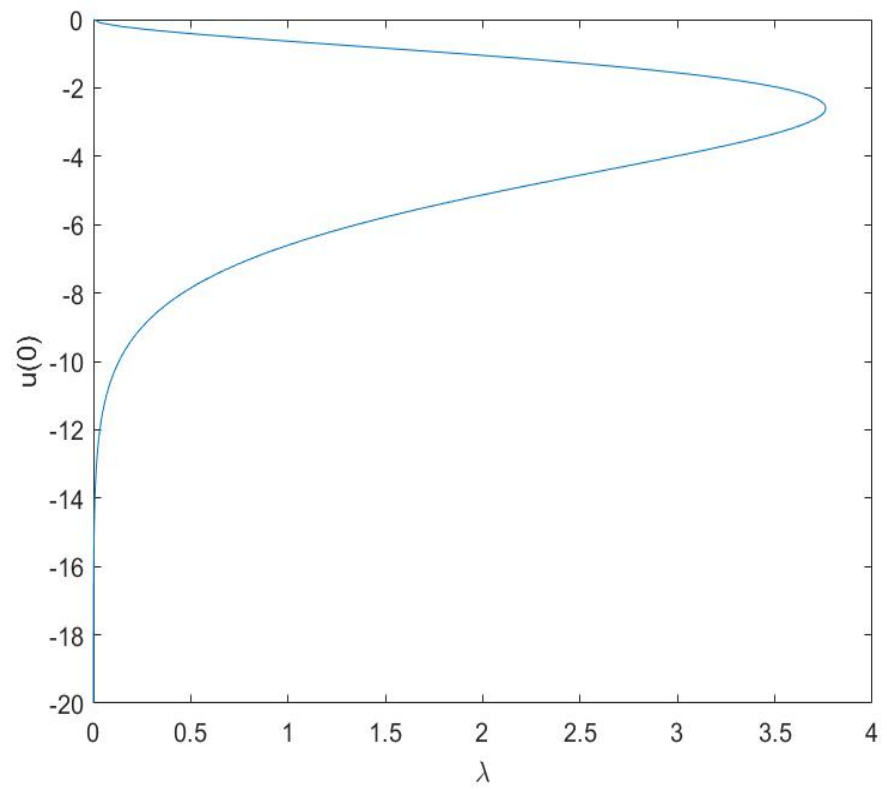


Figure 1: MABG pr ~~...~~ **tion diagram**

2. DIVERGENCE FORMULATIONS OF (MABG)

An alternative formulation to **(MABG)** is given by

$$\mathbf{(MABG.DIV.1)} \quad \left\{ \begin{array}{l} \text{Find } u \text{ } \mathit{convex} \text{ and } \lambda > 0 \text{ such that} \\ \left\{ \begin{array}{l} -\nabla \cdot (\text{cof } \mathbf{D}^2 u) \nabla u = -2\lambda e^{-u} \text{ in } \Omega, \\ u = 0 \text{ on } \partial\Omega, \end{array} \right. \\ \int_{\Omega} (e^{-u} - 1) dx = C. \end{array} \right.$$

In order to take advantage (via **operator-splitting**) of the methodology developed in

R. G., H. Liu, S. Leung & J. Qian, *J. Scient. Comp.*, 2019, for the numerical solution of the **canonical elliptic Monge-Ampère equation**

$$\mathbf{(E-MA)} \quad \det \mathbf{D}^2 u = f (> 0) \text{ in } \Omega, u = g \text{ on } \partial\Omega,$$

we reformulate **(MABG.DIV1)** as

$$\text{(MABG.DIV.2)} \left\{ \begin{array}{l} \text{Find } u \text{ convex, } \mathbf{p} \text{ symmetric positive semi-definite and } \lambda > 0 \text{ s.t.} \\ -\nabla \cdot (\text{cof } \mathbf{p}) \nabla u = -2\lambda e^{-u} \text{ in } \Omega, \\ u = 0 \text{ on } \partial\Omega, \\ \mathbf{p} - \mathbf{D}^2 u = \mathbf{0}, \\ \int_{\Omega} (e^{-u} - 1) d\mathbf{x} = C. \end{array} \right.$$

3. AN ASSOCIATED INITIAL VALUE PROBLEM

We are going to associate with **(MABG.DIV.2)** an *initial value problem* whose *steady state solutions* solve **(MABG)**. After *time-discretization*, the resulting algorithm can be viewed as a nonlinear variant of the *inverse power method with shift* (the shift being here associated with the operator \mathbf{I} / τ , τ being a *time-discretization step*).

(MABG.DIV.2) \rightarrow (MABG.IVP)

Find $u(t) \leq 0$, $\mathbf{p}(t)$ **SPSD** (point wise), $\lambda(t) > 0$ so that :

(MABG.IVP)

$$\left\{ \begin{array}{l} \frac{\partial u}{\partial t} - \nabla \cdot [\varepsilon \mathbf{I} + \text{cof } \mathbf{p}] \nabla u = -2\lambda e^{-u} \text{ in } \Omega \times (0, +\infty), \\ u = 0 \text{ on } \partial\Omega \times (0, +\infty), \\ \frac{\partial \mathbf{p}}{\partial t} + \gamma(\mathbf{p} - \mathbf{D}^2 u) = \mathbf{0} \text{ in } \Omega \times (0, +\infty), \\ \int_{\Omega} (e^{-u} - 1) d\mathbf{x} = 1, \forall t > 0, \\ (u(0), \mathbf{p}(0)) = (u_0, \mathbf{p}_0). \end{array} \right.$$

Above: **(i) $\varphi(t): \mathbf{x} \rightarrow \varphi(\mathbf{x}, t)$. (ii) $\varepsilon > 0$ ($\varepsilon \approx h^2$ in practice). (iii) $u_0 \leq 0$. (iv) $\gamma > 0$. (v) \mathbf{p}_0 **SPSD** (pointwise).**

4. TIME-DISCRETIZATION BY OPERATOR-SPLITTING OF (MABG.IVP)

With $\tau (> 0)$ a *time-discretization step* (*fixed* for simplicity) we approximate (MABG.IVP) by:

$$(0) \quad (u^0, \mathbf{p}^0) = (u_0, \mathbf{p}_0).$$

For $n \geq 0$, $(u^n, \mathbf{p}^n) \rightarrow u^{n+1/3} \rightarrow (u^{n+2/3}, \mathbf{p}^{n+1}) \rightarrow u^{n+1}$ as follows:

First Step: Solve the following (*well-posed*) *linear elliptic problem*

$$(1) \quad \begin{cases} u^{n+1/3} - \tau \nabla \cdot [\varepsilon \mathbf{I} + \text{cof } \mathbf{p}^n] \nabla u^{n+1/3} = u^n & \text{in } \Omega, \\ u^{n+1/3} = 0 & \text{on } \partial\Omega. \end{cases}$$

Second Step:

$$(2)_1 \quad \mathbf{p}^{n+1}(\mathbf{x}) = P_+ \left[e^{-\gamma\tau} \mathbf{p}^n(\mathbf{x}) + (1 - e^{-\gamma\tau}) \mathbf{D}^2 u^{n+1/3}(\mathbf{x}) \right], \text{ a.e. } \mathbf{x} \in \Omega,$$

$$(2)_2 \quad \begin{cases} u^{n+2/3} - u^{n+1/3} = -2\tau\lambda^{n+1} e^{-u^{n+2/3}}, \\ \int_{\Omega} (e^{-u^{n+2/3}} - 1) d\mathbf{x} = C (\Leftrightarrow u^{n+2/3} \in S_C = \{\varphi \text{ measurable, } \int_{\Omega} (e^{-\varphi} - 1) d\mathbf{x} = C\}). \end{cases}$$

Third Step:

(3) $u^{n+1} = \inf(0, u^{n+2/3}).$

Above:

◆ Problem (1) is a very classical *linear elliptic problem*. It has the following property:

$$u^n \leq 0 \implies u^{n+1/3} \leq 0.$$

◆ P_+ is an operator, mapping the space of the 2×2 *real symmetric matrices* onto the *closed*

convex cone of the real SPSD 2×2 matrices (if \mathbf{q} is a 2×2 *real symmetric matrix* with *eigenvalues* μ_1 and μ_2 , $\exists \mathbf{S} \in \mathbf{O}(2)$ s.t. then, operator P_+ is defined by

$$\mathbf{q} = \mathbf{S} \begin{pmatrix} \mu_1 & 0 \\ 0 & \mu_2 \end{pmatrix} \mathbf{S}^{-1};$$

$$P_+(\mathbf{q}) = \mathbf{S} \begin{pmatrix} \max(0, \mu_1) & 0 \\ 0 & \max(0, \mu_2) \end{pmatrix} \mathbf{S}^{-1}.$$

◆ We consider system $(2)_2$ as an *optimality system* associated with the following *minimization problem*

$$(MIN) \quad u^{n+2/3} = \arg \min_{v \in S_C} \left[\frac{1}{2} \int_{\Omega} |v|^2 d\mathbf{x} - \int_{\Omega} u^{n+1/3} v d\mathbf{x} \right] .$$

It follows from (MIN) that $u^{n+2/3}$ is the L^2 -projection of $u^{n+1/3}$ onto S_C . Unless $u^{n+1/3} \in S_C$ problem (MINP) may have no solution since S_C is not weakly closed in $L^2(\Omega)$.
Fortunately its discrete analogues have solutions.

◆ **Algorithm (0) – (3)** has clearly the flavor of an *inverse power method* (with *truncation*).

◆ **Step 3** has been included to be *on the safe side*. Numerical experiments suggest that if *algorithm (0) – (3) is properly initialized, (3) is useless*.

Two important remarks are in order:

Remark 4: *Algorithm (0) – (3)* ‘enjoys’ a **splitting error** forcing us to use a **small time – discretization step τ** .

Remark 5: There is no need to compute λ^{n+1} at each time step. Indeed,

$$\frac{u^{n+2/3} - u^{n+1/3}}{\tau} = -2\lambda^{n+1} e^{-u^{n+2/3}} \Rightarrow (\text{since } u^{n+2/3} \in S_C) \lambda^{n+1} = \frac{\int_{\Omega} (u^{n+1/3} - u^{n+2/3}) d\mathbf{x}}{2\tau(C + |\Omega|)},$$

i.e., λ^{n+1} is obtained by the **ratio of two small numbers**. It is safer (?) to proceed as follows:

Denote by (u_{τ}, p_{τ}) the limit of $(u^{n+1/3}, p^n)_n$. It makes sense to approximate the (nonlinear) eigenvalue λ by

$$\lambda_{\tau} = -\frac{\int_{\Omega} (\varepsilon \mathbf{I} + \text{cof} p_{\tau}) \nabla u_{\tau} \cdot \nabla u_{\tau} d\mathbf{x}}{2 \int_{\Omega} u_{\tau} e^{-u_{\tau}} d\mathbf{x}}$$

a (kind of) **generalized Rayleigh quotient**.

5 . FINITE ELEMENT APPROXIMATION OF (MABG)

Assuming that Ω is a **bounded convex polygonal domain** of \mathbf{R}^2 (or has been approximated by a family of such domains) we introduce a family $(\mathcal{T}_h)_h$ of triangulations of Ω like those in **Figure 2** (h is, typically, the **length of the largest edge(s)** of \mathcal{T}_h). Next, we approximate the functional spaces $H^1(\Omega)$ and $H_0^1(\Omega)$ by

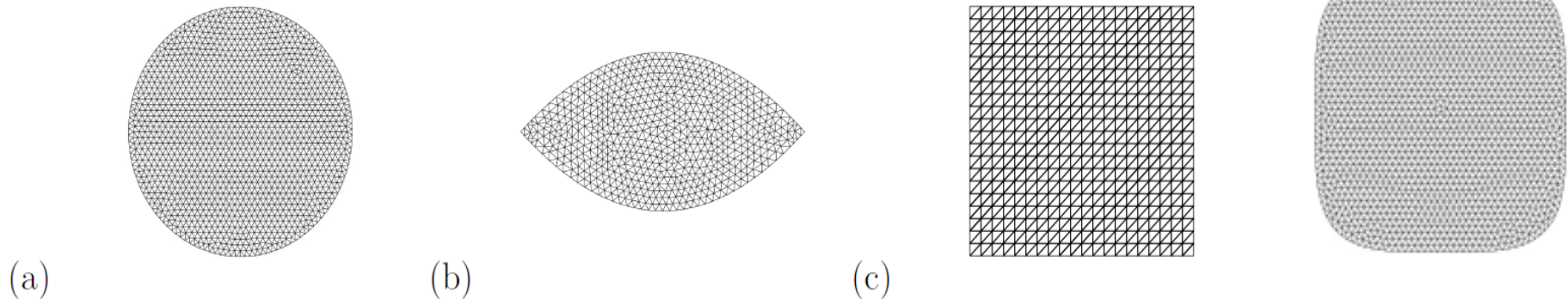
$$V_h = \{\varphi \in C^0(\overline{\Omega}), \varphi|_T \in P_1, \forall T \in \mathcal{T}_h\},$$

and

$$V_{0h} = \{\varphi \in V_h, \varphi|_{\partial\Omega} = 0\} (= V_h \cap H_0^1(\Omega)),$$

respectively, P_1 being the space of the **polynomial functions of two variables** of **degree ≤ 1** .

Figure 2 *Some triangulations*



Let us denote by Σ_h (resp., Σ_{0h}) the set of the *vertices* of \mathcal{T}_h (resp., the set $\Sigma_h \setminus \Sigma_h \cap \partial\Omega$). We have then

$$\dim V_h = \text{Card } \Sigma_h (:= N_h) \text{ and } \dim V_{0h} = \text{Card } \Sigma_{0h} (:= N_{0h}).$$

We assume that the vertices of \mathcal{T}_h have been numbered so that $\Sigma_{0h} = \{Q_k\}_{k=1}^{N_{0h}}$. For $k = 1, \dots, N_{0h}$, we define ω_k as the union of those triangles of \mathcal{T}_h which have Q_k as a common vertex. We denote by $|\omega_k|$ the *measure (area)* of ω_k .

Approximating the *Monge-Ampère part* of the *splitting scheme (0) – (3)* is a (boring) and time

consuming repetition of **RG-HL-TL & JQ, *J. Scient. Comp.*, 2019**. Focusing on the *eigenvalue* part, we approximate S_C by S_{Ch} defined (*trapezoidal rule*) by:

$$S_{Ch} = \{\varphi \in V_{0h}, \sum_{k=1}^{N_{0h}} |\omega_k| (e^{-\varphi(Q_k)} - 1) = 3C\}.$$

The *discrete analogue* of the L^2 – *projection* onto S_C is done by a **SQP** method very easy to implement, showing (as expected) fast convergence properties.

Remark 6: We can take advantage of the fact that τ is *small* by replacing **(MIN)** by **(MIN.LIN)** obtained by *linearization*

$$\mathbf{(MIN.LIN)} \quad u^{n+2/3} = \arg \min_{v \in DS_C^{n+1/3}} \left[\frac{1}{2} \int_{\Omega} |v|^2 d\mathbf{x} - \int_{\Omega} u^{n+1/3} v d\mathbf{x} \right],$$

where

$$DS_C^{n+1/3} = \left\{ v \mid \int_{\Omega} e^{-u^{n+1/3}} (1 + u^{n+1/3} - v) d\mathbf{x} = C + |\Omega| \right\}.$$

The *closed form solution* of **(MIN.LIN)** is given by

$$u^{n+2/3} = u^{n+1/3} + \frac{\int_{\Omega} e^{-u^{n+1/3}} d\mathbf{x} - (C + |\Omega|)}{\int_{\Omega} e^{-2u^{n+1/3}} d\mathbf{x}} e^{-u^{n+1/3}}$$

The above function coincides with the **1st iterate** of the **SQP method** initialized by **$u^{n+1/3}$** .

6. NUMERICAL RESULTS

6.1. TEST PROBLEM FOR THE UNIT DISK

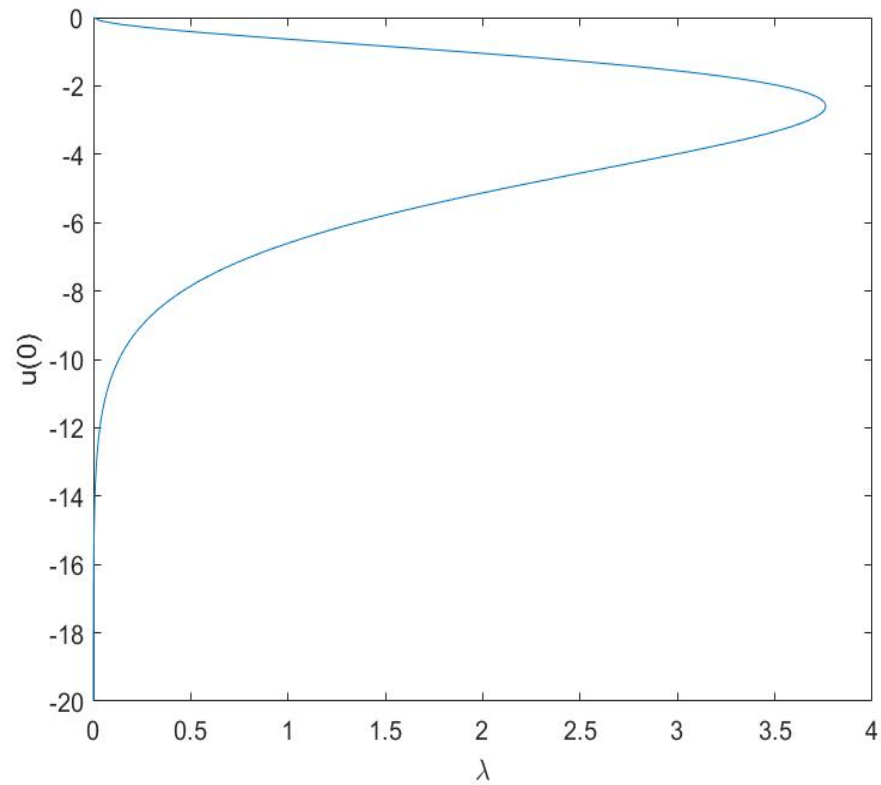


Figure 3: MABG problem on the unit disk: Exact solution bifurcation diagram

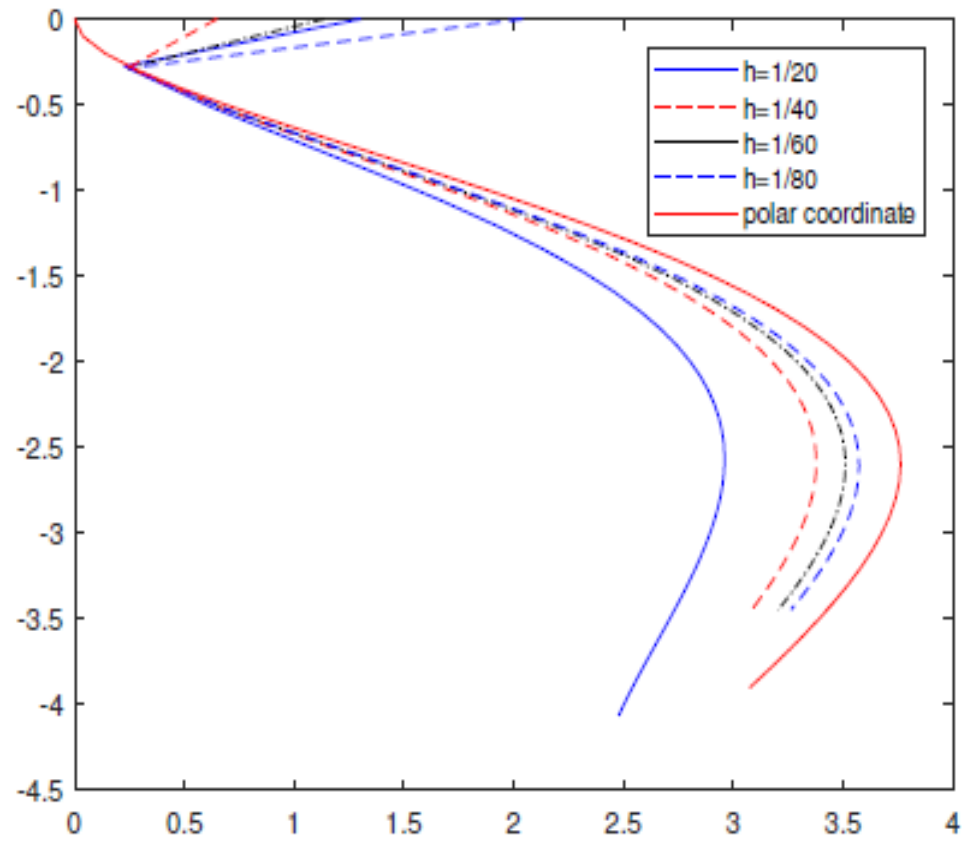
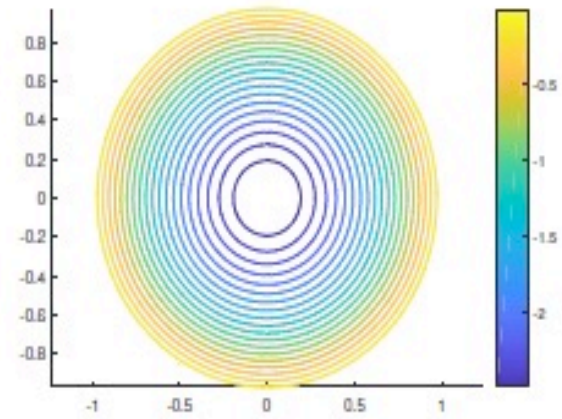
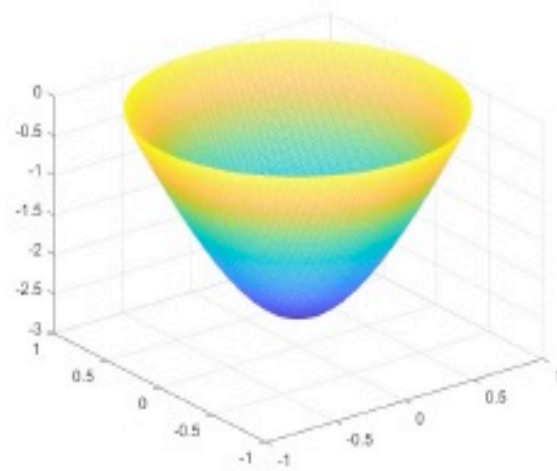


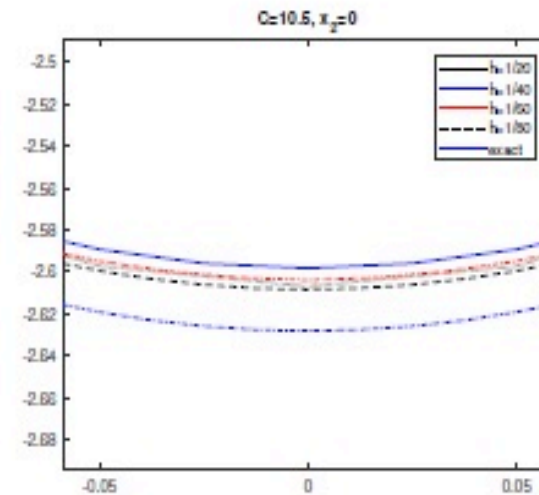
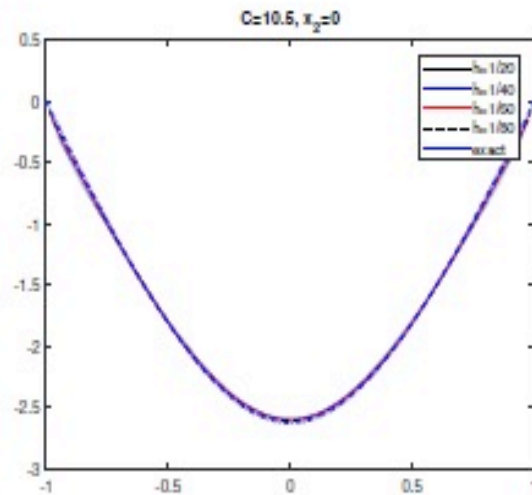
Figure 4: *Bifurcation diagram* comparison for the *unit disk*

The *discrepancy* shown on **Figure 4** for *small values* of C is the result of an *erroneous initialization*. *This mistake has been corrected*. The reason we exhibit these partially wrong results is to show the *robustness* of our methodology. Indeed, without human intervention, our method *'returns quickly by itself'* on the *correct* approximate bifurcation diagrams as C increases.

Figure 5.
Results
at the
exact
turning
point
($C = 10.5$)



(a)



(b)

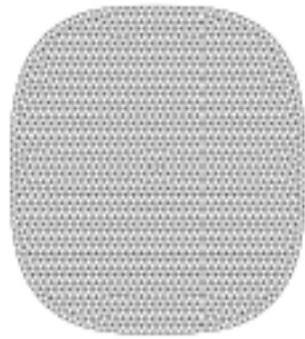
h	$u(0, 0)$	λ
1/20	- 2.5411	2.95
1/40	- 2.5983	3.3773
1/60	- 2.6038	3.5102
1/80	- 2.6084	3.5723
0 ⁽¹⁾	- 2.5950	3.7617

Table 3. MABG problem: Variation with h of the computed turning points

⁽¹⁾ Exact solution

$$\lambda_h - \lambda_0 = \text{quasi-textbook } O(h)$$

6.2. TEST PROBLEMS FOR REGULARIZED SQUARES



(a)



(b)

Mesh for $|(x_1 - 1/2)^q| + |(x_2 - 1/2)^q| \leq (1/2)^q$ with $h = 1/40$: (a) $q=3$. (b)

$q = 4$

FIGURE 6

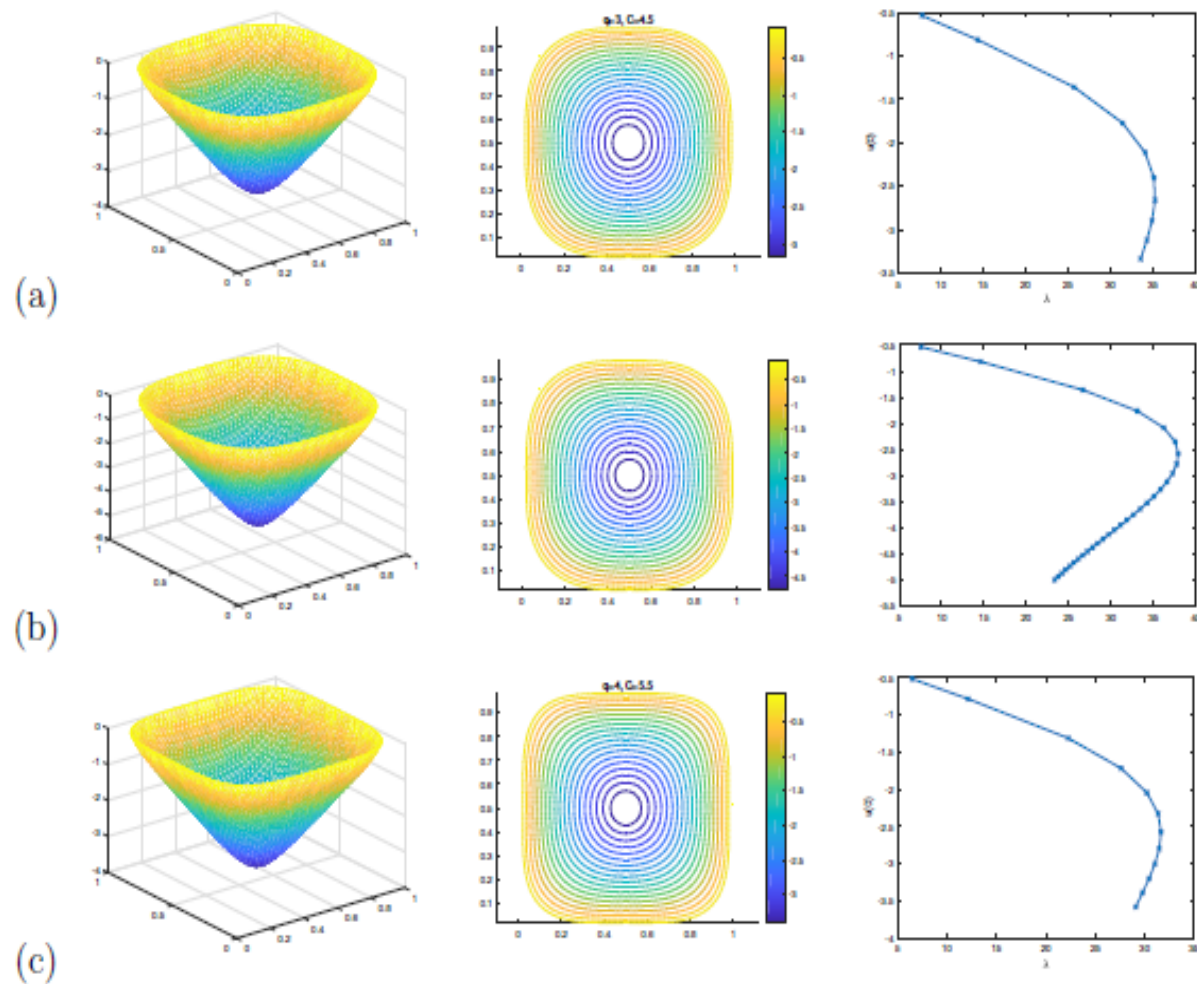


Figure 5: Graph of solution, contour of solution and bifurcation diagram. (a) $q = 3, \Delta t = h^2/2$, with $C = 4.5$. (b) $q = 3, \Delta t = h^2/8$ with $C = 15$. (c) $q = 4, \Delta t = h^2/2$ with $C = 5.5$.

« *il faut essayer, vas-y* »⁽¹⁾

CEDRIC VILLANI

DEA d' ANALYSE NUMERIQUE (Université P. & M. Curie)

Fields Medal 2010

MERCI POUR VOTRE ATTENTION

⁽¹⁾

“ One has to try, let's go ”